JOURNAL OF SOLID STATE CHEMISTRY 100, 262–271 (1992)

Lithium Intercalation into $PbNb_2S_5$, $PbNbS_3$, $SnNb_2Se_5$, $BiVS_3$, $SnVSe_3$, and $PbNb_2Se_5$ Misfit Layer Chalcogenides

L. HERNÁN, J. MORALES, J. PATTANAYAK,* AND J. L. TIRADO

Departamento de Química Inorgánica e Ingeniería Química, Facultad de Ciencias, Universidad de Córdoba, San Alberto Magno s/n, E-14004 Córdoba, Spain

Received November 11, 1991; in revised form February 6, 1992; accepted March 27, 1992

The intercalation of lithium into various misfit layer chalcogenides of two different stoichiometries was performed by using *n*-butyl lithium on powders. The reaction was found to proceed topochemically, and a greater expansion in the *c* direction and higher lithium contents were observed in the lithiated phases with "MM'_2X_5" approximate stoichiometries compared to "$MM'X_3$" stoichiometries. This behaviour difference is assigned to the different stacking sequence of the slices of the two sublattices formed by double layers of MX and sandwiches of $M'X_2$. Lattice distortions are induced during lithiation, leading to changes in the relative orientation of MS-type bilayers and to complete amorphization after long reaction times. The synthesis and partial characterization of a new misfit layer selenide of nominal composition "$PbNb_2Se_5$" is also reported. The value of the *c*-dimension ($c = 37.3_7$ Å) suggests a stacking sequence PbSe–$NbSe_2$–$NbSe_2$–PbSe–$NbSe_2$–$NbSe_2$, etc. This material becomes highly unstable on lithium intercalation and decomposes to its constituents after a few hours of lithiation.

Introduction

Misfit layer chalcogenides—sulfides and selenides—have been the subject of detailed studies in the last few years, and a large number of this type of compounds has been newly synthesized (*1–7*). The compounds studied so far occur in two approximate stoichiometries, viz. $MM'X_3$ and MM'_2X_5 (M: Sn, Pb, Bi, rare earth metals; M': Ti, V, Nb, Ta, Cr; X: S, Se). In the former case, the misfit layer compounds consist of double MX layers (C) with a rock-salt related structure that alternate with one CdI_2-related $M'X_2$ layer (H). For the 1 : 2 : 5 approximate composition, two layers of $M'X_2$ alternate with one MX layer. Usually, both substructures have *a* and *b* parallel axes; however, while the mesh fits along the *b* direction, there is an incommensurate misfit along the *a* direction due to the different *a* dimension (*3–7*) of the two sublattices.

Due to the layered character of these compounds, it can be anticipated their usefulness as hosts for intercalation of electron donating species such as alkali metals (*3*). Recently, we have started to perform a systematic study of the lithium intercalation properties of these materials (*8, 9*). Preliminary results have shown that the incoming lithium ions induce a marked distortion of [MS] slabs compared with [$M'S_2$] layers that undergo small changes. The aim of this paper is to study the reactivity toward lithium intercalation of some recently reported chalcogenides [$SnVSe_3$, $SnNb_2Se_5$ (*8*),

[1] On leave from IIT (Kharagpur, India).

0022-4596/92 $5.00

TABLE I

COMPOSITION, AND X-RAY DIFFRACTION MULTIPLE-ORDER REFLECTIONS OF THE BASAL PLANES OF "$PbNb_2Se_5$"

	%Pb	%Nb	%Se
Experimental	10.2	23.6	66.2
Theoretical for $PbNb_2Se_5$	12.5	25.0	62.6

h k l	d_{obs}(Å)	d_{calc}(Å)	I_{obs}
0 0 6	6.222	6.226	64
0 0 8	4.663	4.669	14
0 0 10	3.730	3.736	23
0 0 12	3.111	3.113	100
0 0 14	2.668	2.668	24
0 0 16	2.334	2.335	17
0 0 18	2.080	2.075	32
0 0 22	1.719	1.698	12
0 0 24	1.559	1.557	57

$BiVS_3$ (*10*), $PbNb_2S_5$ (*11*), $PbNbS_3$ (*12*)] and the "$PbNb_2Se_5$" misfit layer phase recently prepared by our research group, in order to establish the stability ranges and the structure of the lithiated phases. The effect of the different compositions and stoichiometries in the lithiation process is also discussed.

Experimental

Six samples were used as intercalation hosts, the nominal compositions of which were $PbNb_2S_5$, $PbNbS_3$, $SnNb_2Se_5$, $BiVS_3$, $SnVSe_3$, and $PbNb_2Se_5$. Attempts at preparing vanadium compounds with a 1 : 2 : 5 approximate stoichiometry failed. The synthesis and characterization of $SnVSe_3$, $SnNb_2Se_5$ (*8*), $BiVS_3$ (*10*), $PbNb_2S_5$ (*11*), and $PbNbS_3$ (*12*) were reported elsewhere. All samples were obtained by direct combination of the elements (Strem Chemicals), mixed in pellet form, and sealed in silica tubes under vacuum. For "$PbNb_2Se_5$," the tube was heated first at 300°C for 1 day and then at 900°C for 7 days. The sample was reground and reheated at 900°C for another 7 days. The final composition of this sample was determined semiquantitatively by energy-dispersive electron-induced X-ray emission analysis (EDX) on a scanning electron microscope.

Lithium intercalation reactions were performed by the *n*-butyl-lithium technique in a hexane solution (1.6 mol liter^{-1} at room temperature under an inert atmosphere (M. Braun glove-box). Unreacted *n*-butyl-lithium was removed by washing off the product with dry hexane with suction filtering. The lithium content of the samples was determined by atomic absorption spectrometry.

Powder X-ray diffraction data were collected with a Siemens D500 diffractometer by using CuK_α radiation and a graphite monochromator. Electron micrographs were obtained with a JEOL 200 CX instrument.

Results and Discussion

The samples of approximate composition $SnVSe_3$, $SnNb_2Se_5$, $BiVS_3$, $PbNb_2S_5$, and $PbNbS_3$ were obtained as high-purity polycrystalline black powders with metal luster. Their composition, X-ray, and electron dif-

TABLE II

COMPOSITION AND *c* PARAMETER VALUES OF MISFIT PHASES SUBJECTED TO REACTION WITH *n*-BUTYL-LITHIUM FOR DIFFERENT TIMES

System: Reaction time (days)	$PbNb_2S_5$		$PbNbS_3$		$SnNb_2Se_5$	
	Li*	c(Å)	Li*	c(Å)	Li*	c(Å)
0	—	35.6_7	—	23.8_5	—	37.0_9
3	1.8	36.7_6	0.1	23.8_7	0.5	37.2_8
7	2.6	36.7_5	Amorphous		1.7	37.8_7
System: Reaction time (days)	$BiVS_3$		$SnVSe_3$		$PbNb_2Se_5$	
	Li*	c(Å)	Li*	c(Å)	Li*	c(Å)
0	—	22.4_4	—	24.2_0	—	37.3_7
3	0.07	22.4_7	0.5	24.4_2	Decomposed	
7	0.13	22.5_4	Amorphous			

Note. Li*: Lithium per formula unit.

fraction data were consistent with previously reported data and were typical of high-purity samples. For the newly prepared phase "$PbNb_2Se_5$," the atomic Pb, Nb and Se contents found by semiquantitative EDX determination (Table I) were consistent with an approximate 1 : 2 : 5 composition. However, the exact composition could not be determined chemically or spectroscopically, as with other systems (*13*). Precise single-crystal X-ray diffraction determination of the ratio between the *a* unit cell parameters of the two sublattices involved in their structure and the number of MX and $M'X_2$ units in each unit cell yielded the final composition. The powder XRD pattern of "$PbNb_2Se_5$" shows several intense lines which are multiple-order reflections of the basal planes, and few weak lines. The observed and calculated *d*-spacings and relative intensities for each (00*l*) reflection are listed in Table I. From these values, we calculated the *c* unit cell parameter to be 37.3_6 Å. This value is consistent with a unit cell including two C and four H slabs forming an HHCHHC repeating unit along the [001] direction.

The extents of reaction of the six chalcogenide samples treated with *n*-butyllithium for two different times are given in Table II. The reaction proceeded with no gas production, and the crystals lost their silvery black appearance and changed to dark grey. Two findings warrant further comments. First, the rate of lithium intercalation is greater for those compounds with a nominal stoichiometry of 1 : 2 : 5; in fact, compounds with a nominal stoichiometry of 1 : 1 : 3 scarcely prone to intercalate lithium and become amorphous very readily upon lithiation. This different degree of lithium intercalation seems to be more closely associated to the stoichiometry than to the constituent elements and has also been observed in the Pb–Ti–S system (*9*).

This behavior has also been found for other guest molecules such as hydrazine (*14*). In fact, the *c*-spacing of $BiTa_2S_5$ increases markedly on immersion of the chalcogenide in an aqueous hydrazine solution, while no intercalation occurs when $BiTaS_3$ is treated under similar conditions. The structural differences between the two compositions seemingly control both the kinetics of lithium intercalation and the stability of the lithiated phases. Both the "$MM'X_3$" and the "MM'_2X_5" series are made up of 2-atom-thick MX layers (C) and 3-atom-thick $M'X_2$ layers (H) stacked along the *c*-axis, but with different stacking sequences. Thus, an alternating sequence of both CHCHC layers accounts for the structure of "$MM'X_3$," while a model defined by a CHHCHHC sequence has been suggested for the "MM'_2X_5" composition. In fact, the crystal structure for this latter series has only been determined for $(PbS)_{1.14}(NbS_2)_2$ (*11*). A projection of both structures along the *a* axis is shown in Fig. 1.

In both systems, van der Waals forces account for the bonding between the two types of slabs. It is worth noting that the M atoms are not exactly located in the chalcogen atom layer of the MX slab, but they protrude slightly and form outer layers. This means that M atoms are coordinated not only to five X atoms in the MX double layer, but also to chalcogen atoms in the $M'X_2$ layer. This structural feature probably plays a major role in the intercalation process, as it is sensible to assume that the holes where lithium ions occur are located in the van der Waals gaps. In fact, the intercalation of Li^+ between MX and $M'X_2$ might involve the appearance of repulsive forces between this positive charge and that of M^{2+} owing to the partial screening exerted by the chalcogen atoms on this ion, thus hindering intercalation.

This electronic hindrance is apparently absent in the van der Waals gap between $M'X_2$ slabs with vacant interlayer octahedral and tetrahedral holes defined by the packing of chalcogen atoms. These sites

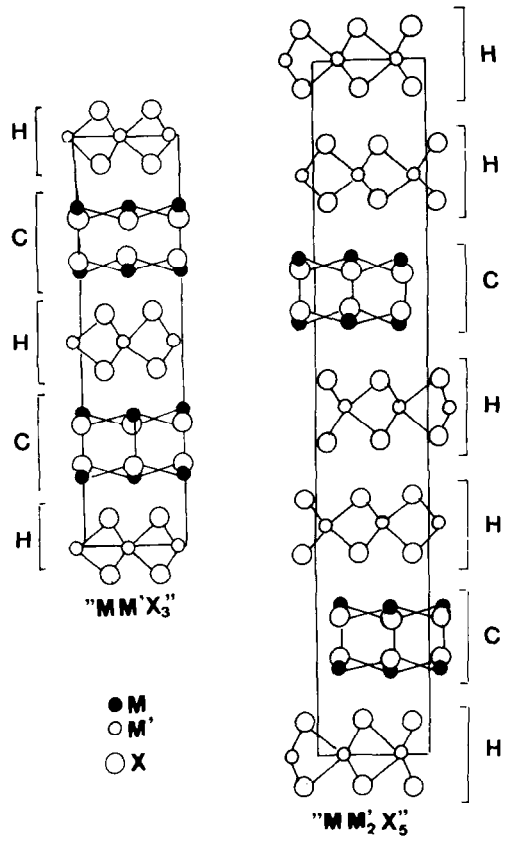

FIG. 1. Idealized projection of the structures of "$MM'X_3$" and "MM'_2X_5" misfit layer compounds along the a axis (from Ref. (7)).

might be occupied by the incoming lithium ions. If these ions were accomodated in the vacant octahedral sites within the van de Waals gap, then the composition of the lithiated phase would be one Li atom per formula unit, MM'_2X_5. However, the lithium content is always greater than one (see Table II) and approaches 2 Li/MM'_2X_5 (*15*). The large value of $PbNb_2S_5$, lithiated for 7 days, is probably the result of the high degree of amorphization of this sample. The location of the remaining Li atoms is uncertain. Various positions are available in this respect. Tetrahedral holes within the van der Waals gap are less prone to be occupied because of the strong repulsive forces between neighbouring positive ions. Similar problems for lithium location shows the phase Li_2TiS_2 obtained by electrochemical lithium intercalation and whose XRD pattern can be indexed in the same symmetry than $LiTiS_2$ (*20*). However, multiple-ion occupancy has been suggested to account for the high lithium contents of some systems (*16*). Thus, the location of Li^+ ions in vacant tetrahedral sites has been suggested for 3D hosts such as spinel structures. In fact, a neutron diffraction study of the discharge product $Li_{12}[Mn_2O_4]$ has shown that the lithium ions reside on both tetrahedral and octahedral sites of the diffusion network (*21*). The other accomodation alternative would be between MX (C) and $M'X_2$ (H) layers. If this is so, then it is difficult to understand the behaviour of the $MM'X_3$ series the degree of lithium intercalation of which is rather low. Probably, kinetic reasons and structural differences account for the degree of lithium intercalation observed.

On the other hand, band structure calculations for misfit layer compounds have not yet been carried out. However, it has been suggested that the NaCl-type unit MS (C) acts as an electron donor part to the $M'S_2$ (H) slab, with the M atom tending to a valency of +3 (*22, 23*). Taking into account that the Nb atoms are surrounded by a slightly distorted trigonal prism of sulfur atoms (D_{3h} symmetry), the splitting of d orbitals results in three levels $a'_1(d_{z^2})$, $e'(d_{xy}, d_{x^2-y^2})$ and $e''(d_{xz}, d_{yz})$. Thus, this configuration would allow at least the uptaking of one mole of lithium per Nb atom, yielding intercalates of nominal composition $LiMM'X_3$ and $Li_2MM'_2X_5$. If the restriction imposed by the electron donor properties of the M atoms is also taken into account, it seems clear that the degree of lithium intercalation is more limited in HCHC phases than in HHCHH.

One other finding of interest is the change observed in the interlayer spacing, c, the

only lattice parameter that can be determined reliably from the powder X-ray diffractometry measurements in phases with misfit structures. Its variation is usually taken as an indirect proof to ascertain the intercalation of guest species into the host structure. The values of this parameter are collected in Table II. The most salient finding in this respect is the marked expansions of the 1 : 2 : 5 series, whereas the lithiation process hardly affects the interlayer spacing of 1 : 1 : 3 phases. Thus, this behavior gives no evidence supporting the hypothesis that Li^+ is intercalated into the chalcogenides. However, we have some additional experimental evidence of the Li^+ intercalation into the structure. Although these measurements are still incomplete, they shed some light on the insertion of lithium. Thus, no intercalation occurred when $SnVSe_3$ was soaked in a solution of *n*-hexyl-amine. By contrast, a significantly increased *c*-spacing was observed when the lithiated chalcogenide was soaked in a similar solution. Moreover, electrochemical lithiation of $PbVS_3$ shows that one equivalent of lithium can be intercalated without destroying its layer structure. These results support the hypothesis that lithium is indeed intercalated in the reaction of *n*-butyl-lithium with the chalcogenides.

On the other hand, while the insertion reaction yields one-phase products in Sn VSe_3, $BiVS_3$, $PbNb_2S_5$, and $PbNbS_3$, as shown by XRD measurements (see Figs. 2A–B and E–F), the diffraction patterns of lithiated 1 : 2 : 5 selenides $SnNb_2Se_5$ (Figs. 2 C–D) and $PbNb_2Se_5$ are typical of mixed phases. In the former case, the XRD pattern of the original sample (Fig. 2C) shows intense *h*00 (a = 25.2$_3$ Å) and 00*l* lines (c = 37.0$_9$ Å), while the sample lithiated for 3 days (Fig. 2D) shows double lines in the positions where multiple-order reflections of the basal spacing would be expected. The first set of lines is consistent with the presence of unlithiated phase, while the second

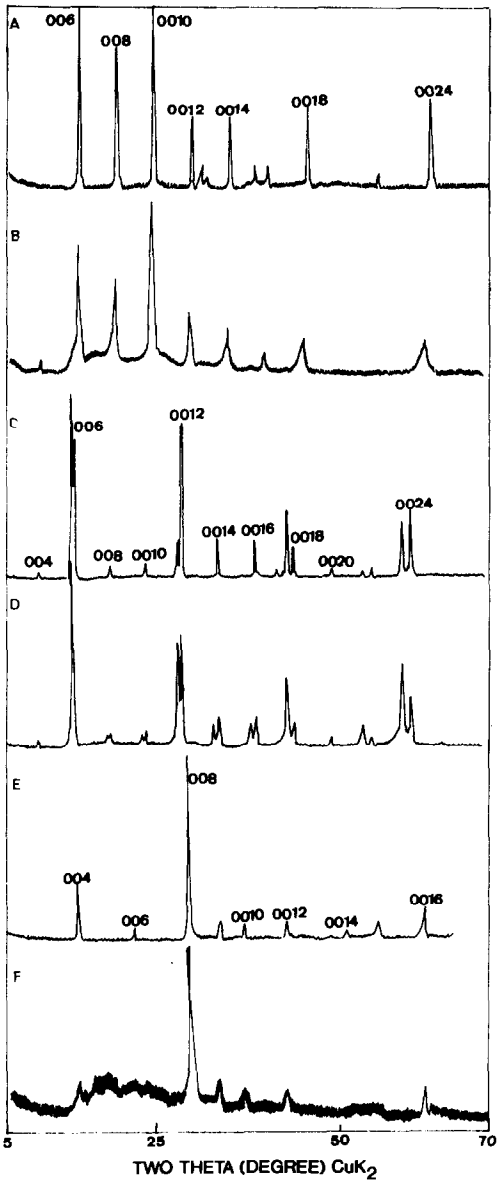

FIG. 2. Powder X-ray diffraction patterns of $PbNb_2S_5$ (A), $SnNb_2Se_55$ (C), $SnVSe_3$ (E) and the products obtained by 3-day lithiation (B, D, and F, respectively).

leads to the c parameter of the lithiated phase (37.2$_8$ Å) given in Table II. This behavior implies the co-occurrence of both unlithiated and lithiated phases, in contrast with the gradual conversion shown by the

sulfide systems. This biphasic mechanism which is similar to those reported for some thermal decomposition reactions (*17*), probably arises from a major distortion induced by lithium intercalation in this system, which does not allow the entire particle to be intercalated. Thus, the particles may collapse in partially lithiated domains, thereby hindering uniform distribution of lithium in the initial particles. In addition, the fact that two phases are present in the 3-day lithiated phase affects the interpretation on the lithium contents shown in Table II. Thus, the lithiated phase derived from $SnNb_2Se_5$ has a content higher than 0.5, which is the average in the biphasic product. This in turn is consistent with the above conclusion that 1 : 2 : 5 phases allow higher lithium contents than 1 : 1 : 3 phases.

For $PbNb_2Se_5$, the sample obtained after 3 hr of lithiation was a mixture of phases that included traces of a partially lithiated misfit layered phase, PbSe and $NbSe_2$. Electron diffraction patterns were used to confirm the presence of these crystalline modifications in the powder sample. From the above results, it seems likely that 1 : 2 : 5 misfit layer selenides are less prone to intercalate lithium in the redox process used in this study. The higher stability of PbSe ($\Delta G_f^\circ = -24.6$ Kcal mole^{-1}) as compared with SnSe ($\Delta G_f^\circ = -21.7$ Kcal mole^{-1}) (NBS Technical note 270-3, 1968) leads to the formation of this product and $NbSe_2$ when the starting solid is $PbNb_2Se_5$. By contrast, in $SnNb_2Se_5$, only the size of the domains is affected.

Additional evidence of the misfit layer structure of the compounds studied here and the structural changes induced by lithium intercalation were obtained by careful observation of the particles under the electron microscope. Figures 3A–F show typical electron diffraction patterns for $PbNb_2S_5$, $PbNbS_3$, $SnNb_2Se_5$, $BiVS_3$, $SnVSe_3$, and $PbNb_2Se_5$ platelike particles, respectively, with an incident beam parallel to [001]. These patterns are typical of misfit layered compounds with alternating H and C or HH and C sublattices. However, these zone-axis electron diffraction patterns do not allow one to distinguish each structural type (HHC or HC).

In all phases, the MS sublattice features a virtually regular cubic pattern in the ab plane of the [001] zone as a result of very similar a and b values and $\gamma \simeq 90°$. Virtually all the particles observed showed a single orientation of the C sublattice. However, multiple orientations of H or C layers have been reported in distorted regions of samples of misfit layer compounds (*18, 19*). Only in $SnNb_2Se_5$ did scarce distorted regions show a pattern like that depicted in Fig. 3C. This intricate pattern can be intepreted in terms of two orientations of the $NbSe_2$ H layers differing by 30°. Other intricate variants with three different orientations of the MS sublattice (C_1, C_2, and C_3, each differing by 60° from the others) were only observed in scarcely distorted regions of the samples.

In addition, the electron diffraction pattern of $BiVS_3$ (Fig. 3D) shows the presence of low-intensity satellite spots surrounding the diffraction spots that are typical of the BiS C sublattice. These spots may be related to the presence of antiphase domain boundaries perpendicular to the a_c axis. In $BiTaS_3$, the presence of such modulation may be the result of a valence disproportionation of the low-stability oxidation state +2 of bismuth into Bi^{+1} and Bi^{+3} (*18*).

In contrast with the patterns discussed above, the vast majority of the particles of the lithiated samples showed the typical patterns in Figs. $3A_L$–E_L. Samples lithiated for short periods develop an apparent 12-fold symmetry, which can be interpreted by considering the stacking of cubic lamella in C_1, C_2, and C_3 orientations, while the H sublattice remains in a single orientation. Since the three orientations are energetically equivalent, the intensities of each set of dif-

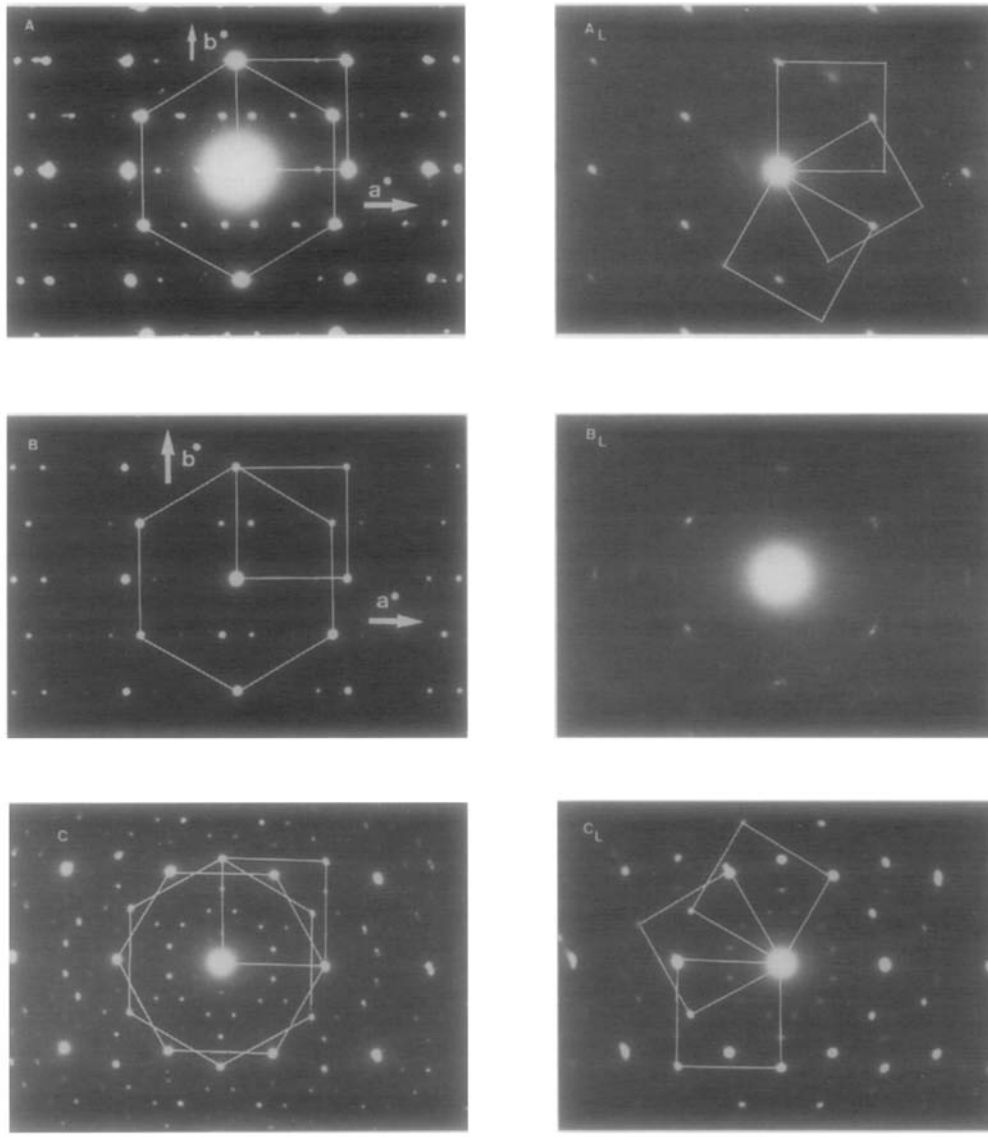

FIG. 3. [001] zone electron diffraction patterns of $PbNb_2S_5$ (A), $PbNbS_3$ (B), $SnNb_2Se_5$ (C), $BiVS_3$ (D), $SnVSe_3$ (E), and $PPbNb_2Se_5$ (F) and samples obtained by 3-day lithiation (A_L–E_L, respectively).

fraction spots are similar. In $BiVS_3$, the 12 spots have satellites due to the above-mentioned antiphase boundaries, thus showing that they are derived from different orientations of C sublattices.

These changes can be interpreted in terms of the distortions induced by introducing Li cations between H and C sublattices. The origin of the preferred distortion of the C sublattice can be ascribed to the interactions of the incoming Li^+ ions with the *M* ions in C layers. These cations are coordinated to five sulfur or selenium atoms in the C sublattice to form roughly a square pyramide. In

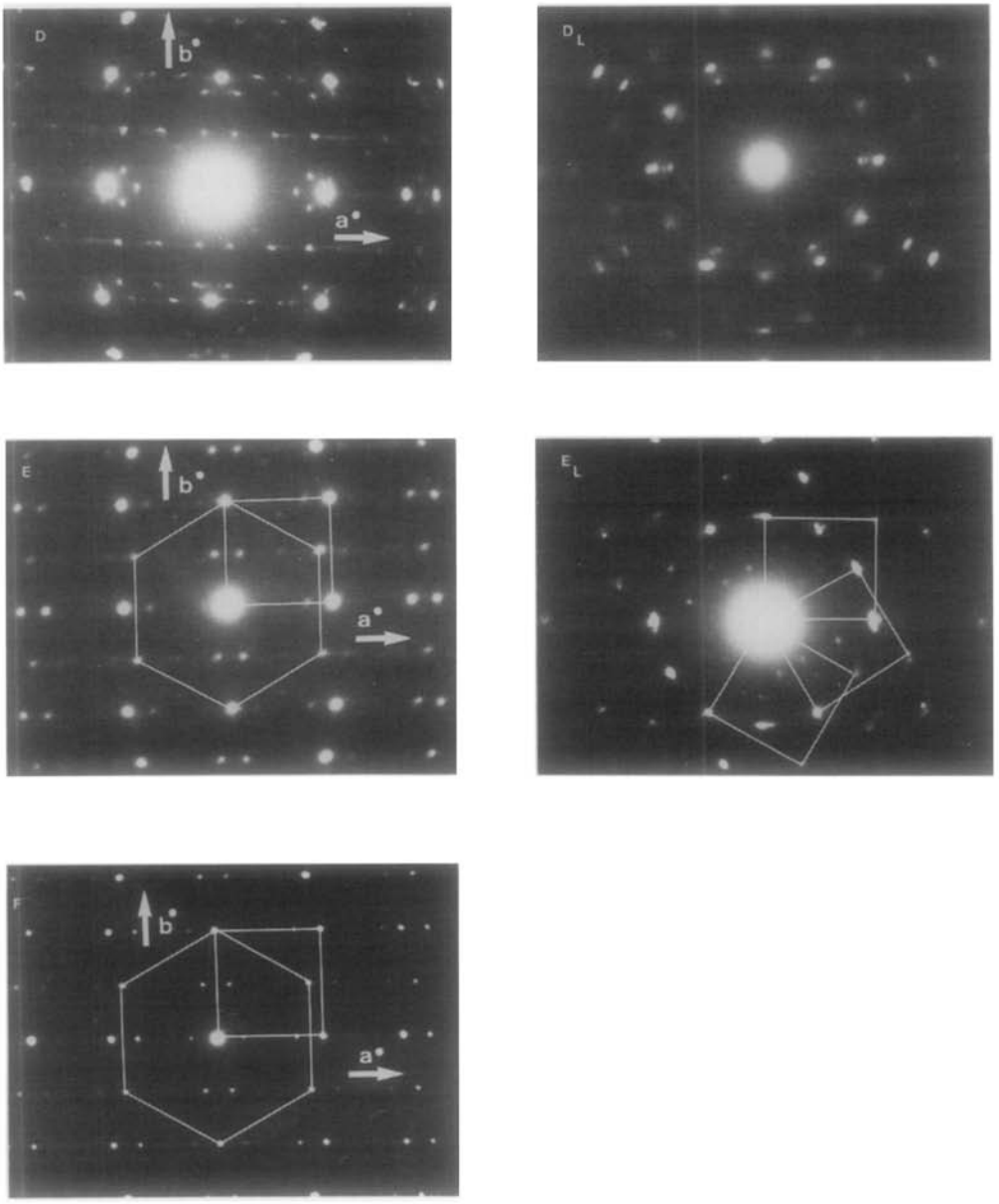

FIG. 3—*Continued*

addition to these five S or Se atoms, each M^{2+} ion is also coordinated to other chalcogen atoms in the neighboring $M'S_2$ or $M'Se_2$ slab. Thus, the intercalation of Li^+ between C and H slabs would shift the M^{2+} ions to the apex of the square pyramid as a result of the strong repulsive forces between the two positive charges. Therefore, Li intercalation between C and H layers may displace both sublattices, as a result of the repulsions between the two positive charges. By contrast, the transition ions are sandwiched be-

tween two S atom sheets, so they do not interact directly with the incoming Li^+ ions. In fact, a charge transfer from Li atoms to transition metal atoms probably takes place via the valence orbitals of the sulfur atoms. The distorting effects induced in the $M'X_2$ layers could be less marked and only extensive reduction of the transition metal would cause the structure collapse for this reason.

On more prolonged treatment, the cubic sublattice spots disappear and only a sixfold symmetry derived from the H sublattice is observed. Diffuse streaks and Debye circles indicate that the C sublattice layers are completely disoriented, so they yield no coherent diffraction. Finally, H spots disappear gradually as the lithium content is increased until a nearly-amorphous state is reached. Thus, at a certain critical concentration of Li ions, the long-range order of C lamellae starts to collapse, whereas H lamellae in the $M'S_2$ sublattice remain unaltered (Fig. 2). This is probably a result of the higher interaction potential of H lattices compared to C lattices, which arises from stronger Coulomb interactions of metal ions with the formal +4 oxidation state. If the process is continued, the systems finally reach a completely disordered state with a diffuse scattering pattern arising from the presence of excess Li ions.

Conclusions

Misfit layer chalcogenides of $MM'X_3$ and MM'_2X_5 approximate stoichiometries are adequate hosts for lithium intercalation reactions. This is shown by the reaction with *n*-butyl-lithium, which takes place topochemically leading to new lithiated phases.

Lattice distortions are induced after short periods of reaction, which consist of an enhanced misorientation of the H and C sublattices. For $BiVS_3$, the presence of satellite spots due to antiphase domain boundaries in the C sublattice is maintained after misorientation of the sublattices. Prolonged lithiation leads to a complete amorphization of the solids.

MM'_2X_5 phases allow higher lithium contents and more pronounced increase in the unit cell *c* parameter as compared with $MM'X_3$ phases. This is the result of the presence of consecutive H layers separated by weak van der Waals interactions in the former case. In addition, the electron donating possibilities of the nontransition metal to the transition metal bands limits the amount of intercalated lithium and this effect is less marked for HHCHHC than HCHC phases.

A newly prepared misfit phase "$PbNb_2Se_5$" is described on the basis of an HHCHHC staking unit. This compound is unstable to lithiation, probably due to the higher thermodynamical stability of PbSe, as compared with PbS, SnS, or SnSe.

Acknowledgments

The authors express their gratitude to Fundación Ramón Areces, C.I.C.Y.T. (MAT 88-0708) and P.F.C.T.E.E. (J. Pattanayak) for financial support.

References

1. L. Guemas, P. Rabu, A. Meerschaut, and J. Rouxel, *Mater. Res. Bull.* **23,** 1061 (1988).
2. G. A. Wiegers, A. Meetsma, S. Van Smaalen, R. J. Haange, J. Wulff, Th.J. Zeinstra, J. L. De Boer, S. Kuypers, G. Van Tendeloo, J. Van Landuyt, S. Amelinckx, A Meerschaut, P. Rabu, and J. Rouxel, *Solid State Commun.* **70,** 409 (1989).
3. G. A. Wiegers, A. Meetsma, R. J. Haange, and J. L. De Boer, *Solid State Ionics* **32/33,** 183 (1989).
4. I. Goto, M. Gotoh, K. Kawagachi, I. Oosawa, and M. Onoda, *Mater. Res. Bull.* **25,** 307 (1990).
5. G. A. Wiegers, A. Meetsma, R. J. Haange, and J. L. De Boer, *J. Solid State Chem.* **89,** 328 (1990).
6. K. Suzuki, T. Enoki, and K. Yneada, *Solid State Commun.* **78,** 73 (1991).
7. G. A. Wiegers and A. Meerschaut, *J. Less-Common Met.*, in press.
8. L. Hernan, J. Morales, J. Pattanayak, and J. L. Tirado, *Chem. Lett.*, 1981 (1991).
9. L. Hernan, P. Lavela, J. Morales, J. Pattanayak, and J. L. Tirado, *Mater. Res. Bull.* **26,** 1211 (1991).

10. Y. Gotoh, M. Onoda, K. Uchida, and Y. Tanaka, *Chem. Lett.*, 1559 (1989).
11. A. Meerschaut, L. Guemas, C. Aunel, and J. Rouxel, *Eur. J. Solid State Inorg. Chem.* **27,** 557 (1990).
12. G. A. Wiegers, A. Meetsma, R. J. Haange, S. Van Smaalen, J. L. De Boer, G. Van Meerschaut, P. Rabu, and J. Rouxel, *Acta Crystallogr. Sect. B* **46,** 324 (1990).
13. J. Wulff, A. Meetsma, R. J. Haange, J. L. De Boer, and G. A. Wiegers, *Synth. Met.* **39,** 1 (1990).
14. Y. Oosawa, Y. Gotoh, and M. Onoda, *Chem. Lett.*, 1583 (1989).
15. P. Lavela, J. Morales, and J. L. Tirado, *Chem. Mater.*, **4,** 2 (1992).
16. M. Figlarz, *Prog. Solid State Chem.* **19,** 1 (1989).
17. F. Fievet and M. Figlarz, *J. Catal.* **39,** 350 (1975).
18. S. Kuypers, J. Van Landuyt, and S. Amelinckx, *J. Solid State Chem.* **86,** 212 (1990).
19. S. Kuypers, G. Van Tendeloo, J. Van Landuyt, and S. Amelinckx, *Acta Crystallogr. Sect. A* **45,** 291 (1989).
20. J. R. Dahn, M. A. Py, and R. R. Haering, *Can J. Phys.* **60,** 307 (1982).
21. W. I. F. David, M. M. Thackeray, L. A. De Picciotto, and J. B. Goodenough, *J. Solid State Chem.* **67,** 316 (1987).
22. G. A. Wiegers, A. Meetsma, R. J. Haange, and J. L. De Boer, *Mater. Res. Bull.* **23,** 1551 (1988).
23. J. Wulff, A. Meetsma, S. Van Smaalen, R. J. Haange, J. L. De Boer, and G. A. Wiegers, *J. Solid State Chem.* **84,** 118 (1990).